International Journal of Nanomedicine

Dovepress
open access to scientific and medical research

Open Access Full Text Article

ORIGINAL RESEARCH

RETRACTED ARTICLE: Formulation for the Targeted Delivery of a Vaccine Strain of Oncolytic Measles Virus (OMV) in Hyaluronic Acid Coated Thiolated Chitosan as a Green Nanoformulation for the Treatment of Prostate Cancer: A Viro-Immunotherapeutic Approach

Faiza Naseer[1,2], Tahir Ahmad[1], Kousain Kousar[1], Salik Kakar[3], Rabia Gul[2], Sadia Anjum[4], Usman Shareef[2]

[1]Industrial Biotechnology, Atta-ur-Rehman School of Applied Biosciences, National University of Science and Technology, Islamabad, Pakistan; [2]Shifa College of Pharmaceutical Sciences, Shifa Tameer e Millat University, Islamabad, Pakistan; [3]Healthcare Biotechnology, Atta-ur-Rehman School of Applied Biosciences, National University of Science and Technology, Islamabad, Pakistan; [4]Department of Biology, University of Hail, Hail, Saudia Arabia

Correspondence: Faiza Naseer; Tahir Ahmad, Email faiza.naseer@ymail.com; tahir@asab.nust.edu.pk

Background: Oncolytic viruses are reported as dynamite against cancer treatment nowadays.

Methodology: In the present work, a live attenuated oral measles vaccine (OMV) strain was used to formulate a polymeric surface-functionalized ligand-based nanoformulation (NF). OMV (half dose: not less than 500 TCID units; 0.25 mL) was encapsulated in thiolated chitosan and outermost coating with hyaluronic acid by ionic gelation method characterizing parameters was performed.

Results and Discussion: CD44 high expression was confirmed in prostatic adenocarcinoma (PRAD) by GEPIA which extracted data of normal and cancer tissue from GTEx and TCGA. Bioinformatics tools confirmed the viral hemagglutinin capsid protein interaction with human Caspase-I, NLRP3 and TNF-α and viral fusion protein interaction with COX-II and Caspase-I after successful delivery of MV encapsulated in NFs due to high affinity of hyaluronic acid with CD44 on the surface of prostate cancer cells. Particle size = 275.6 mm, PDI = 0.37 and ±11.5 zeta potential were shown by zeta analysis, while the thiolated group in NFs was confirmed by FTIR and Raman analysis. SEM and XRD showed a spherical smooth surface and crystalline nature, respectively, while TEM confirmed virus encapsulation within nanoparticles, which makes it very useful in targeted virus delivery systems. The virus was released from NFs in a sustained but continuous release pattern till 48 h. The encapsulated virus titer was calculated as 2.34×107 TCID50/mL units, which showed syncytia formation on post-day infection 7. Multiplicities of infection 0.1, 0.5, 1, 3, 5, 10, 15, and 20 of HA-coated OMV loaded NFs as compared to MV vaccine on PC3 was inoculated with IC50 of 5.1 and 3.52, respectively, and growth inhibition was seen after 72 h via MTT assay which showed apoptotic cancer cell death.

Conclusion: Active targeted, efficacious, and sustained delivery of formulated oncolytic MV is a potent moiety in cancer treatment at lower doses with safe potential for normal prostate cells.

Keywords: green synthesis, controlled release, immunotherapeutic agent, in vitro studies, oncolytic activity, oncolytic measles virus, prostate cancer, targeted virus/drug delivery system, thiolated chitosan, tumour targeting, vaccine-based nanoformulation

Introduction

Prostatic adenocarcinoma (PaC) is the second most commonly diagnosed adenocarcinoma globally after lung cancer in elderly males, accounting for approximately 2 million new cases per annum and a quarter of all cancers.[1] The metastatic

Received: 6 September 2022
Accepted: 25 October 2022
Published: 9 January 2023

Graphical Abstract

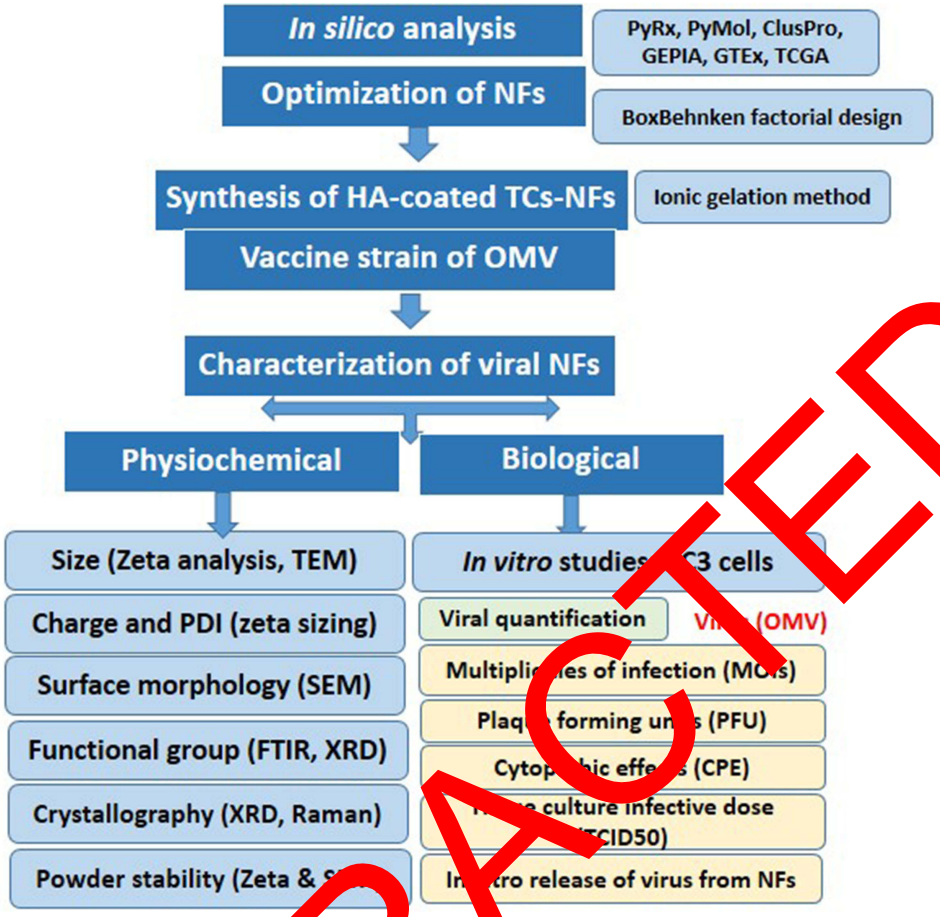

PaC remains unresponsive to the currently available therapies, despite all advances. The efficacies of available conventional therapies are compromised due to low tumor specificity, off-target toxicity profile, a less bioavailable drug for desired therapeutic outcomes, and piecemeal tumor eradication, which can be overcome by employing targeted oncolytic virus delivery of NF-based therapeutic approaches.[2,3] The nanoscale moieties (<1,000 nm) are extremely welcoming for diagnostic and therapeutic modalities in acute and chronic phases of various diseases including cancers. Their small size, surface modifications by specific ligand binding, and release of enclosed drug in a sustained manner allow them to show specificity towards a target, high safety, better solubility, and bioavailability with potent action which are vital objectives for efficacious cancer therapies. These therapies include NFs of OVs which was not yet extensively studied, and are under consideration in clinical trials for multiple cancers including PaC.[4] Oncolytic viruses, such as parvovirus H1, reovirus, vaccinia virus, Edmonston-derived strains of the MV, and several strains have revealed the therapeutic potential for the treatment of various human malignancies and are commonly known as dynamite for cancer cells in this era.[5] The efficacy and pharmacological activity of the oncolytic activity of viruses depend on the selectivity of cancer cells and increased cytotoxicity at specific sites leads to immunological action against cancer cells with the expression of various antigens coupled with danger-associated and pathogen-associated molecular patterns (DAMPs and PAMPs) and cytokines of specific tumors. These markers ultimately improve the prognosis and overall survival of sufferers.[6]

After proving exceptional preclinical anticancer potential with safety profiles, many oncolytic viruses including MV show efficacious pharmacological activity as a potent therapeutic moiety for the treatment of various types of cancer. The live attenuated vaccine strain of OMV, ie, Leningrad-16, is with a remarkable array of oncolysis and lack of genotoxicity.

Its immunogenicity is proven in the early phases of clinical trials that data support its safety and efficacy.[7] MV, a negative-strand RNA virus of the genus Morbillivirus belongs to the Paramyxoviridae family and causes the highly contagious but common, acute measles disease. The length of the genome is approximately 16 kb, which encodes six structural and two non-structural proteins. The viral glycoproteins hemagglutinin and fusion mediate receptor cause binding and fusion at the plasma membrane, respectively. The wild-type MV binds with CD150/SLAM and epithelial nectin-4 receptors on lymphoid cells while the vaccine strains of OMV infect cells primarily via receptors CD46. Because there is some kind of mutations in the receptor attachment glycoprotein hemagglutinin (H) in vaccine strain, resulting in the high affinity of H for CD46 resulting in syncytia formation as a typical cytopathic effect that ultimately undergoes apoptotic death of specific cancer cells.[8] The vaccine strain of MV is not infectious to normal cells because of a mutation in H-protein which is involved in viral attachment with cells and its entry.

One of the limitations to the administration of oncolytic viral vectors is their delivery. The effective way to deliver OMV at the specific tumor site is to use cell carriers. The naturally available biocompatible polymers after thiolation (TCs) and hyaluronic acid (HA) are commonly used to date for the formulation of targeted viral delivery. These are biodegradable polysaccharides with several functional moieties for surface functionalization.[9] They create the virus without degrading its oncolytic action and prepare sustained/controlled release formulation. These polymers can bind and can present on the mucous layer via physical interactions including covalent and non-covalent bonds and electrostatic forces because of the covalently bound but free and active form of thiol groups. The mechanistic behavior of Cs was enhanced after crosslinking with covalent or ionic bond formation among anionic molecules like tripolyphosphate polyanions (TPP).[10] There is no addition of any expensive/harsh chemicals, with less expenditure of energy, and produce environmentally gentle formulations by the process known as green synthesis of virus-encapsulated nanoparticles via the Ionic Gelation method. The ionic gelation method involves binding between molecules based on electrostatic forces of attraction between oppositely charged molecules. Also, this is a green synthesis approach as its using raw material extracted from a biological source, not using any acids/organic solvents, there are no toxic by-products involved and therefore it is the most preferred method of chemically synthesizing nanoparticles which come with a plethora of side effects for the environment and also complex methodologies.[11,12] One of the majorly utilized negative charge cross-linkers like TPP acts as a linking agent in the formulation of nanoparticles that are used with great therapeutic outcomes in the treatment of various diseases.[13]

Hyaluronic acid is a hydrophilic mucopolysaccharide and carries a negative charge. Its functionally reactive sites provide the carboxylic acid group, glucuronic acid group, N-acetyl group, and primary and secondary hydroxyl groups, which plays role in the conjugation of suitable ligands, cross-linking of bioactive compounds, and give this polymer the flexibility of modification, which makes it highly favorable for therapeutic purposes. CD44 is a receptor that is highly expressed on cancer cells, particularly in solid tumors like prostate cancer, breast cancer, cervical cancer, and glioblastoma. CD44 plays a crucial role in cancer initiation, invasion, and metastasis. It also plays a critical role in chemotherapy resistance.[14] According to previous research the mechanism of reactive oxygen species (ROS) production, the proliferation of P[illegible] cells and the glycolytic pathway (glucose metabolism) are mediated by CD44 receptors and its high expression is linked with cancer aggression.[15] Upon binding with its high-affinity ligand HA, it forms a ligand-receptor (L-R) complex which is internalized by the cellular endocytosis pathway, followed by the pH-sensitive release of the virus encapsulated in the HA enclosed nanosystem inside the cancer cell.[16] In recent studies, the potential of HA for the biocompatible delivery of viruses to target tumor sites is being extensively exploited due to the targeted interaction of this polymer with CD44 on cancerous cells.[17]

The major objective of the current research was to formulate the novel sustained/controlled and targeted viral delivery system with the outermost coating of ligand for surface-functionalization by encapsulating weak attenuated measles virus by following measures of green synthesis. This NF targeted the cancer cells actively after selective attachment with receptor CD44, protecting the virus from antibody-mediated clearance. Release of the oncolytic virus by following receptor-mediated endocytosis at tumor cells as a potent oncolytic immunotherapeutic agent is a highly effective approach to bypassing off-target toxicities and for gaining the highest desired on-target pharmacological effect as shown in schematic flow in Figure 1.

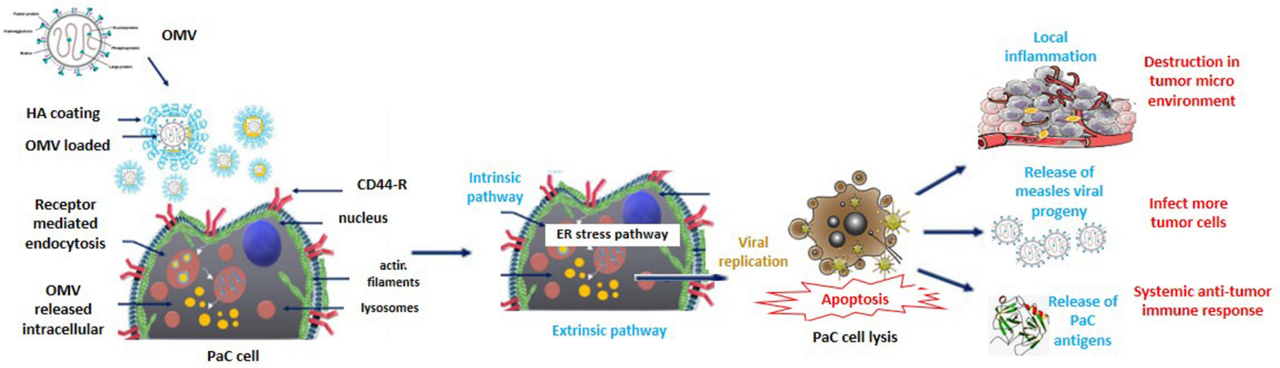

Figure 1 Schematic illustration of PaC cells uptake and intracellular trafficking of OMV-loaded NFs with HA-CD44 (L-R) binding at a specific site to induce oncolysis as an oncolytic viro-immunotherapeutic agent.

Methodology

Materials

Thioglycolic acid (TGA), Tripolyphosphate polyanions (TPP), and low molecular weight Thiolated Chitosan (Cs) (50–190 kilodaltons), with 70–80% deacetylation were purchased from Scharlau (Germany). Glacial acetic acid, Dipotassium hydrogen phosphate, Sodium dihydrogen phosphate, Hydroxylamine, Calcium chloride ($CaCl_2$), Potassium dihydrogen phosphate, and Sodium hydroxide (NaOH) were ordered from Merck (Germany). High molecular weight hyaluronic acid (HA) 1,500 kd, high retention dialysis membrane (12,000–14,000 Mw cut off), Sodium borohydride, and artificial mucin were ordered from Sigma-Aldrich USA and provided by Science Home store, Islamabad, Pakistan. The Virology and immunology lab, Atta-ur-Rehman School of Applied Biosciences (ASAB), National University of Science and Technology (NUST), Islamabad, Pakistan has provided distilled water and some solvents and chemicals of analytical grade.

CD44 Expression by Bioinformatics Analysis

Bioinformatics tool GEPIA (Gene Expression Profiling Interactive Analysis) was used to analyze the expression of targeted receptor CD44 in normal prostate and PaC tissues. GEPIA (http://gepia.cancer-pku.cn) extracts normal tissue and tumor data from the GTEx (Genotype-Tissue Expression) and TCGA (The Cancer Genome Atlas).

Protein–Protein Docking Analysis

After confirmation of L-R (L=HA; R=CD44) binding with the previous study, in silico analysis of viral and host cells, P-P interaction was explored by using ClusPro (2.0) and PyMOL (1.8). ClusPro is used for protein–protein docking servers which use three different steps, namely rigid body docking, and clustering based on root mean square deviation (RMSD) of approximately 1,000 lowest energy structures and energy minimization to exclude the steric clashes.[18] PyMOL was used for the manual inspection of proteins (downloaded from PDB) and afterward for the analysis of protein–protein interactions.[19]

The viral targeted proteins were hemagglutinin (H) and viral fusion protein (F). Both of the proteins are a type of glycoproteins that are part of the viral capsid, while the H protein acts as the receptor binding site.[20] Sequence for both the proteins was extracted from the protein data bank (PDB.com) (PDB ID: 2RKC for H and PDB ID: 5YXW for F) and was inspected manually by PyMOL. The host cell proteins, namely Tumor necrosis factor (TNFα) (PDB ID: 1CA4), Cyclooxygenase II (COX-II) (PDB ID: 1CX2), Caspase-I (PDB ID: 6BZ9), and NLR family pyrin domain containing 3 (NLRP3) (PDB ID: 7PZD) because they are most abundant cells and when interacted with foreign proteins such as viral proteins can stimulate the immune response to the cancer cell death.[21,22] The weighted energy scores for all the interactions are shown in Table 1.

Preparation Method Optimization for NF

The central composite design was selected by Design of Expert (DOE) version 8.0.6.1 following the factorial design of BoxBehnken to get the results for an optimized NF (Table 2). The dependent variables as responses included the particle size of NF, the polydispersity index (PDI), and zeta potential. An optimized formulation was selected, and further

Table 1 Weighted Energy Scores for Host and Viral P-P Interactions

Sr. #	Name of Receptor Protein	Name of Ligand Protein	Weighted Energy Scores in KJ/mol	Obtained From
1	Caspase-I	Measles virus Hemagglutinin	−1,071.2	ClusPro
2	NLRP3	Measles virus Hemagglutinin	−1,218.9	ClusPro
3	TNFα	Measles virus Hemagglutinin	−1,283.6	ClusPro
4	COX-II	Measles virus fusion protein	−1,290.8	ClusPro
5	Caspase-I	Measles virus fusion protein	−1,066.4	ClusPro

characterizations were carried out. The ligand concentration (HA), polymer solution (TCs), and oncolytic measles virus (OMV) were variable by keeping the concentration of cross-linker solutions (TPP) constant.

Oncolytic Measles Virus (OMV) Strain

A stock solution of 1×10^{12} plaque forming units (PFU) in PBS of live attenuated measles virus vaccine Edmonton strain vaccine was courteously provided by the National Institute of Health (NIH), Islamabad, Pakistan. This was extracted from the Connaught strain, a strain of measles virus derived from the same original isolate as other vaccine strains, such as Schwarz after 69 passages in avian leucosis-free chick embryo fibroblast cultures. All vials were stored at −80°C and every time ice was used for thawing before each experiment.[23]

Table 2 Concentrations of Variables Including Ligand (HA), Polymer Solution (TCs), and Oncolytic Measles Virus (OMV) for the Development of OMV-Loaded NFs

Std	Run	Factor 1	Factor 2	Factor 3	Response 1	Response 2	Response 3
		A: HA conc (mg)	B: TCs conc	C: OMV (dose)	Particle Size (mm)	PDI	Zeta Potential ±mV
8	1	5.00	5.50	1.00	1683	1	−24
7	2	0.50	5.50	1.00	614	0.401	13.8
12	3	2.75	10.00	1.00	680.4	0.416	4.88
3	4	0.50	10.00	0.55	736.1	0.528	13.3
10	5	2.75	10.00	0.10	463.9	0.363	16.4
5	6	0.50	5.50	0.10	393.1	0.472	12
11	7	2.75	1.00	1.00	387.3	0.591	−23.7
1		**0.50**	**1.00**	**0.55**	**275.6**	**0.372**	**11.5**
6	9	5.00	5.50	0.10	396.2	0.524	−25.6
14	10	2.75	5.50	0.55	339	0.363	18.1
4	11	5.00	10.00	0.55	752	1	28.5
2	12	5.00	1.00	0.55	438	0.678	−29.6
13	13	2.75	5.50	0.55	740	0.468	5.65
9	14	2.75	1.00	0.10	416	0.584	−25.7

Note: The bold values show the concentration of chemicals for the formulation of HA-coated OMV-loaded TCs.

Preparation of Polymer and Cross-Linking Agent Solutions

The 0.1% TCs (polymer) solution was prepared with distilled water and 0.1 mg/mL TPP (cross-linker) was dissolved in distilled water for optimized formulation by following the ionic gelation method and green synthesis. Once dissolved, distilled water was used for dilution and filtered through a 0.22 mm filter to make a stock solution of 0.4% chitosan (w/v, 4 mg/mL) with a viscosity of 2.5460.1 centi Poise (cP) as measured using a Model DV-III plus Programmable Rheometer (Brookfield Engineering Laboratories, Middleboro, MA). The formulation was sonicated by using a probe sonicator at 30 mA for 3 minutes. The 0.5 mg/mL HA was used for the outermost coating around the formulation, it was then centrifuged, lyophilized, and further stored at 4°C.[24]

Preparation of OMV-Loaded NF

After the slight modification, the OMV-loaded NFs were formulated by following the green synth[illegible]otocol via the ionic gelation cross-linking method. The solution of 1.0 mg TCs and half a dose of OMV (1 d[illegible] contains [illegible] less than 1,000 TCID units of MV) was added in distilled water by syringe drop by drop with continuous s[illegible]ring at 550 [illegible]m for 10 minutes. The TPP 0.1 mg/mL was added for 15 minutes with uninterrupted stirring at 5[illegible]0 rpm re[illegible]lting i[illegible]he NFs of various strengths at room temperature and the same step was repeated in the prepara[illegible]n of bl[illegible]k NFs. [illegible]ese NFs were named HA-coated OMV-loaded TCs.

Characterization of OMV-Loaded NFs

Physiochemical and Morphological Properties of NFs

Several properties of HA-coated OMV-loaded TCs-NFs were eva[illegible]ated for their imm[illegible]ent characteristics as an active targeted moiety in cancer therapeutics. The size of particles, PDI, [illegible]nd zeta pote[illegible]ial was determined by zeta analysis, and surface morphology and shape were checked by scanning electron [illegible]icroscopy [illegible]EM), transmission electron microscopy (TEM), and Raman analysis. The functional groups we[illegible] explored [illegible]y Fou[illegible]r-transform infrared spectroscopy (FTIR) and X-ray diffraction analysis (XRD). The thermal stabi[illegible]ty wa[illegible]valuated by differential scanning calorimetry (DSC). All assays were performed according to the protocols mei[illegible]o[illegible]d in a previous study.[24]

Viral Quantification from Prep[illegible]red N[illegible]Fs

The method used for counting the n[illegible]mbe[illegible]f [illegible]ruses present/encapsulated in the NFs falls into various categories depending upon the viral activated [illegible]nfectious) [illegible] non-activated (non-infectious) progeny.[25]

Plaque Forming Assay (PFA)

This assay is used to coun[illegible]istinct infectious [illegible]rogeny from the samples containing the virus. The serial dilutions have been made, and, for each di[illegible]ion, ali[illegible]ots were poured into a culture dish of PC3 cells which was covered by an agarose layer. This agarose layer was re[illegible]o[illegible]d and ce[illegible]s were stained to visualize plaque in the cell monolayer at 72 hours post-infection, as shown in Fig[illegible]e 2. The fi[illegible]ings [illegible] assays were stated as plaque-forming units (PFU) per measured volume.[26]

Tissue Cu[illegible]re In[illegible] Dose (TCID50)

Following the [illegible]d–Muench protocol, the viral titre was calculated by measuring 50% TCID. The 1:10 titer solutions of dried OMV-loaded [illegible]Fs with dilution ratio 10^{-2} to 10^{-11} were prepared in PBS buffer 10 µL at pH 7.2. The 96-well plates of PC3 cells at a seeding density of 0.5×10^{4} cells per well were immunized with 10X serial dilution of OMV-loaded NFs and put in 5% CO_2 incubation at 37°C. The total number of infected and uninfected units at several dilutions on the post-day infection 7 (p.d.i) were counted and this titre was reported as TCID50 per mL, also known as endpoint dilution assay, as shown in Figure 3. The amount of sample in one TCID50 is equal to that infecting 50% of the testing sample. PC3 cells inoculated with OMV served as positive control while PC3 cells with growth media only served as a negative control.[27]

Cytopathic Effects (CPE)

The cell morphology analysis helps us to determine the physiological changes a cell undergoes following exposure to specific treatment in a time-dependent and dose-dependent manner. The OMV-loaded NFs as compared to pure MV were added to

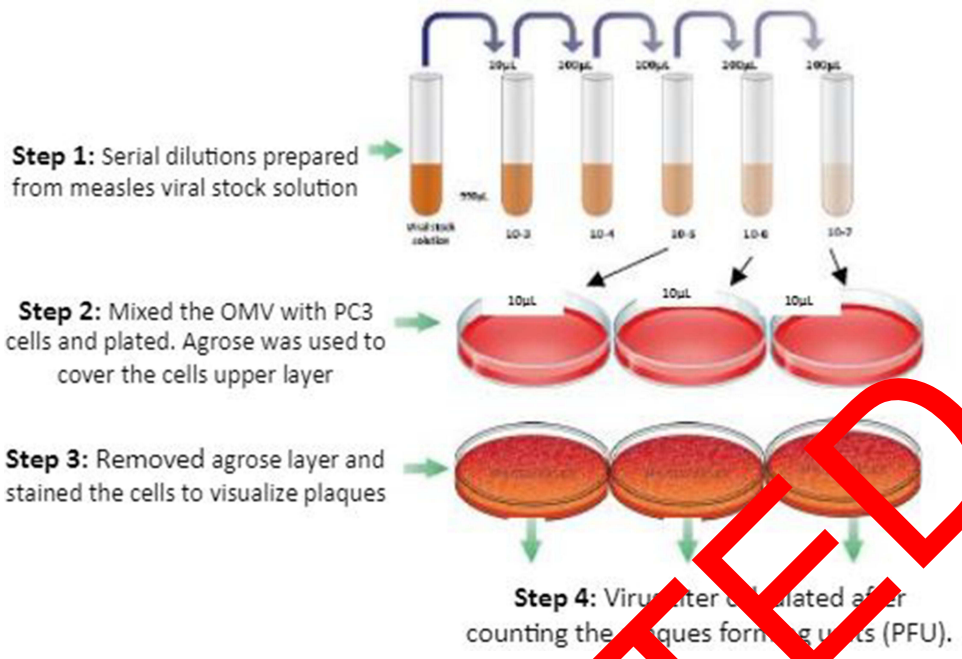

Figure 2 Schematic diagram of determining the virus titer by Plaque forming assay (PFA) after infecting the PC ells with serial dilutions of OMV stock solution.

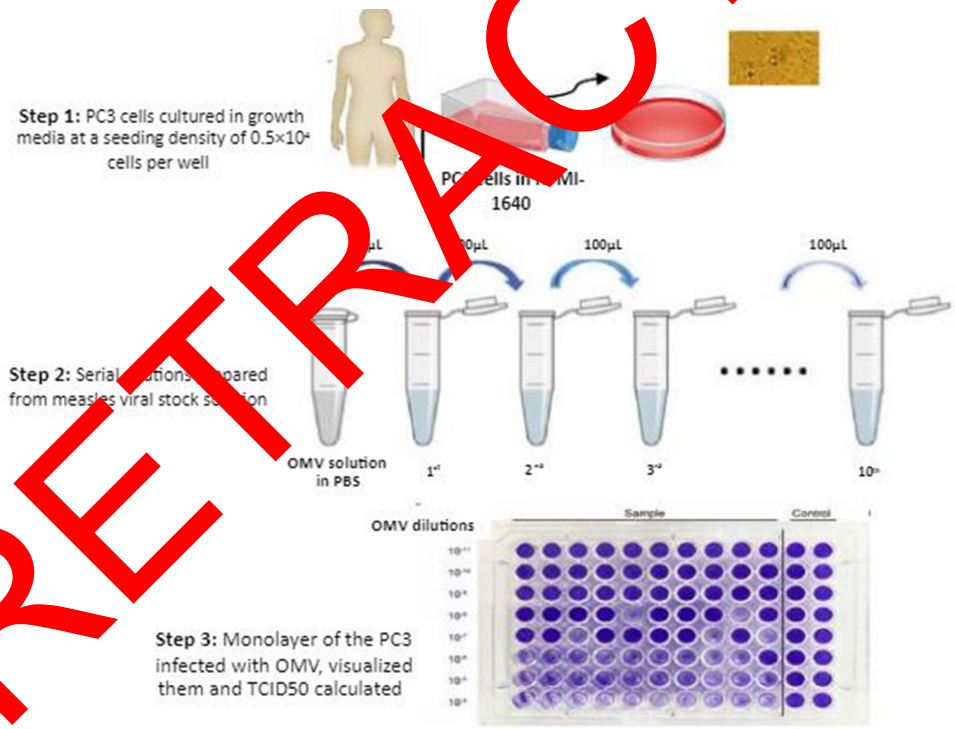

Figure 3 Calculation of TCID50 for OMV-loaded NFs by following Reed–Muench protocol with the help of 1:10 serial dilution of viral solution in PBS.

PC3 cells at different dilutions in a 6-well plate and incubated in 5% CO_2 at 37°C after draining the growth medium from the confluent monolayers. The cells were washed with PBS and replenished with a growth medium after incubation with a virus formulation for 24 hours.[28] The cells were observed for morphological changes including rounding, disaggregation, erosion from the culture plate, and/or vacuolization in the cell layers at p.d.i 7. The cytopathic effects (CPE) were observed by inverted phase contrast microscopy after 12 and 24 hours exposure (TCM-400, OEM-Optical, Labomed, USA).

Multiplicity of Infection (M.O.I.)

The 6-well plates were prepared at the growth surface of a seeding density of 2×10^6 cells/10 cm^2. The prepared OMV-loaded NFs and OMV vaccine strain were inoculated at 0.1, 0.5, 1, 3, 5, 10, 15, and 20 in cells. The plates were incubated for 2 hours just to make the virus adhere to the cells. The cells were washed twice with serum-free DMEM to remove the unattached virus. After that, the cells were incubated in 5% CO_2 at 37°C for 3 days.[26]

In vitro Release of Virus from NFs

The lyophilized HA-coated OMV-loaded TCs-NFs 0.1 g was poured into the dialyzing membrane and put in the PBS 50 mL at pH 7.2. The dissolution assembly was kept at 100 rpm on a magnetic hot plate for continuous stirring at 37°C. The 1.5 mL samples after specified time interims, ie, 0, 0.5, 1, 2, 4, 8, 10 12, 24, 36, and 48 h, were collected from the mixture and centrifuged at 10,000 g/min. These samples were spectrophotometrically analyzed at 595 nm to study the virus release from NFs. The time taken for the release of the virus at the X-axis and the accumulative release amount at the Y-axis was plotted to get the OMV release curve.

In vitro Anti-Cancer Activity

The in vitro anti-cancer activity of OMV-loaded NFs in comparison with the commercially available vaccine strain of OMV was assessed on prostate cancer cells taken from the 62-year-old male bone metastasis of grade IV PaC, termed as PC3, which is an androgen receptor-independent cell line. The cells were generously given by Prof. Dr. Saeed Khan, Department of Molecular Pathology, Dow University of Health Sciences, Ojha Campus Karachi, Pakistan, and cultured in tissue culture flasks of 75 cm^2.[29]

Cell Viability Analysis of OMV-Loaded NFs

The growth inhibition of OMV vaccine strain solution and OMV-loaded NFs were checked by following a previously published protocol with slight amendments. These cells were cultured in 96 well plates with a seeding density of 1×10^4 in each well and put in a humidified atmosphere of incubation with 95% air and 5% CO_2 at 37°C to get the desired confluent layer of cells at their exponential growth phase. The media RPMI-1640 was used to culture the cells along with the 1 mM sodium pyruvate, 2 mM l-Glutamine, 4.5 g glucose/L, and 1.5 g/L sodium bicarbonate, 10% fetal bovine serum (FBS), and 500 µL of Penicillin Streptomycin (pen strep).[30]

The trial was distributed into two treatment groups. Group 1: OMV vaccine strain solution (positive control), and Group 2: HA-coated OMV-loaded NFs as compared to Blank (negative control). MOIs (0.1, 0.5, 1, 3, 5, 10, 15, and 20) of the OMV-loaded NFs as compared to the OMV vaccine strain on PC3 cells were used. After an incubation period of 72 hours, the MTT assay was performed. The growth inhibition (GI) and IC50 were determined as a proportion of viable cells following infection with the measles virus compared to control cells that were not exposed to the virus.

Stability Parameters

The stability-related parameters like zeta analysis and surface morphology of HA-coated OMV-loaded NFs and OMV vaccine strain were analyzed over a period of 3 months while keeping them at conditions of 4°C and room temperature of 37°C.

Statistical Studies

The outcomes taken/calculated from the experiments were analyzed by statistical tools including one-way analysis of variance (ANOVA) and Student's *t*-test with a significant $P\leq0.05$ with the mean values of multiple readings and standard deviation (mean±SD).

Outcomes

CD44 Expression in PaC vs Normal Prostate Tissues

The CD44 expression in prostate adenocarcinomas (PRAD) compared to GTEx and normal TCGA data using the web server GEPIA. The dot-plot data showed clear up-regulation of CD44 as shown in Figure 4.

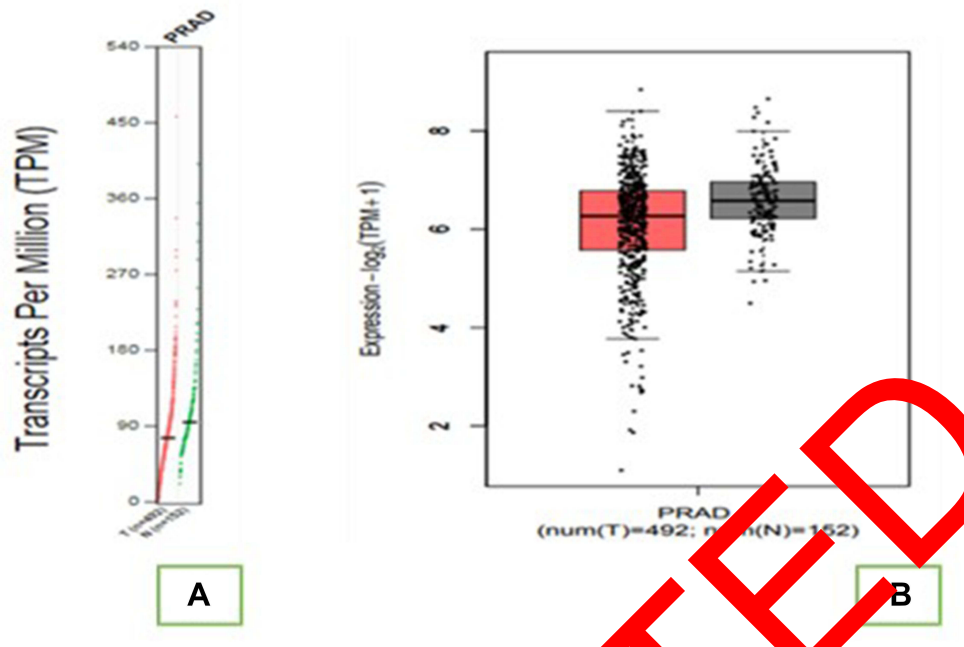

Figure 4 (**A**) TCGA tumor data (red) and its associated normal and GTEX data (green) were given. N: nor T: tumor; Y-axis: transcripts per million (log2(TPM+1)); X-axis: number of normal and tumor samples. (**B**) A GEPIA box plot showed a difference in the expression of 44 in normal (N=152) vs tumor tissues (T=492) and showed visible high expression of CD44 in PaC tissues.

Interpretation of Protein–Protein Docking nalysis

In silico analysis showed the attachment of HA with the C 44-R at bi ding sites A & B from NFs of HA-coated TCs in prostate cancer cells.[23] After confirming t successfu y, the host and viral protein–protein docking studies were performed for several different protei of in t but only the most significant interactions have been discussed below.

Measles Viral Hemagglutinin and H man C pase-I, P Interaction

Figure 5A showed the P-P inte ctions exhibits only polar contacts between the proteins. The type of polar interaction included both hyd en bondin and ionic interactions. There were 10 polar contact points between the proteins. His-271 of the H ain is contact wi Thr-180 of the Caspase-I chain with a bond distance of 2A°. Likewise, all contact point intera on distances within the acceptable range indicating the strong bonding between the proteins. The amino acid int actions long with the distances are shown in Table 3.

Table es vir hema utinin and human caspase-1 interactions and distances

S.#	Ar no Acid (Receptor Protein)	Amino Acid (Ligand Protein)	Distance (A°)	Type of Interaction
1	ASP-297	GLN-248	2.0	Polar
2	G-383	GLU-277	2.2, 2.7	Polar
3	ARG-383	TYR-214	1.9	Polar
4	ASP-288	ARG-212	1.8, 1.9	Polar
5	GLU-250	ASN-200	2.4	Polar
6	ARG-178	PRO-263	1.9, 2.0	Polar
7	THR-180	HIS-271	2.0	Polar

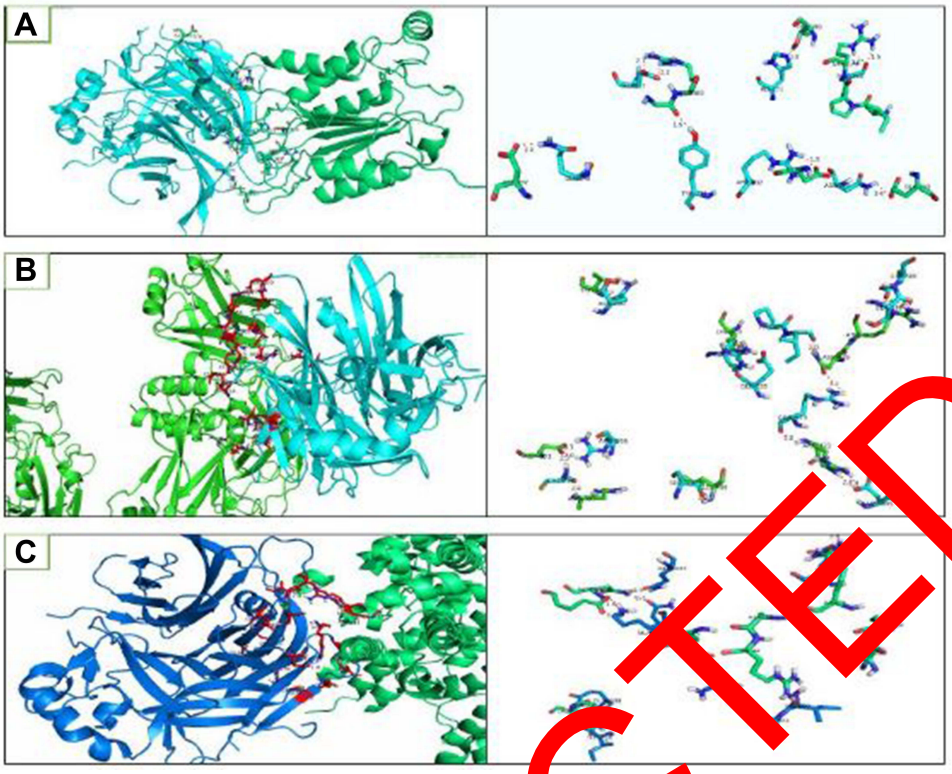

Figure 5 The interaction between Caspase-I (**A**), TNF (**B**), and NLRP3 (**C**) indicated by Gree[illegible]icks and Viral H[illegible]otein by Blue sticks. The complete P-P interactions with the side chain are shown on the left side of the figure.

Measles Virus Hemagglutinin and Human T[illegible]P-P Int[illegible]action

Figure 5B shows the P-P interactions [illegible]d exhi[illegible]ts onl[illegible] polar contacts between the proteins. Several of the arginine residues were involved in both hydr[illegible]ding and ionic interaction. There were 14 polar contact points between the proteins. All [illegible]f the c[illegible]tact point interaction distances are within the acceptable range, indicating strong bonding betw[illegible]e proteins, [illegible]s shown in Table 4.

Table 4 Measles [illegible]us hema[illegible]glutinin and human TNF-alpha interactions and distances

Sr.#	Ami[illegible] Acid [illegible]ceptor Pro[illegible]in)	Amino Acid (Ligand Protein)	Distance (A°)	Type of Interaction
1	[illegible]R-499	ASN-200	1.9	Polar
2	ASP-[illegible]	ARG-195	2.0, 2.1	Polar
3	ASP-351	CYS-606	2.2	Polar
4	ARG-385	CYS-606	2.4	Polar
5	LYS-493	ARG-556	1.7	Polar
6	LYS-493	GLU-535	1.7	Polar
7	ASN-439	ILE-559	2.0	Polar
8	LEU-498	SER-550	2.8	Polar
9	ARG-423	ASP-505	2.5, 1.8	Polar
10	ARG-440	GLU-389	1.8	Polar
11	ARG-440	SER-588	2.4	Polar
12	ASN-439	ARG-533	3.3	Polar

Measles Virus Hemagglutinin and Human NLRP3, P-P Interaction

Figure 5C shows the P-P interactions and exhibits only polar contacts between the proteins. The most significant interaction in this was between the majority of glutamine residues of both receptor and ligand proteins. There were 11 polar contact points between the proteins. All of the contact point interaction distances are within the acceptable range, indicating strong bonding between the proteins, as shown in Table 5.

Table 5 Measles virus hemagglutinin and human NLRP3 interactions and distances

Sr.#	Amino Acid (Receptor Protein)	Amino Acid (Ligand Protein)	Distance (A°)	Type of Interaction
1	GLN-35	GLN-248	1.9	Polar
2	GLN-35	ILE-238	2.6	Polar
3	GLN-45	GLN-278	2.3	Polar
4	GLN-45	GLN-334	1.9	Po
5	SER-5	GLN-225		Po
6	GLU-293	ARG-7	1.9, 2.8	Polar
7	GLU-15	ARG-261	8, 2	Polar
8	ARG-12	ILE-260	1.9,	Polar

Interpretation via BoxBehnken Factorial Design

The dependent variables such as nanoparticle size, the PDI, and zeta potential were measured via Design of Expert (DOE) version 8.0.6.1 for optimization of HA-coated OMV-loaded NF, as shown in Table 2, and the parameters related to the selected formulation were displayed by BoxBehnken factorial design, as shown in Figure 6.

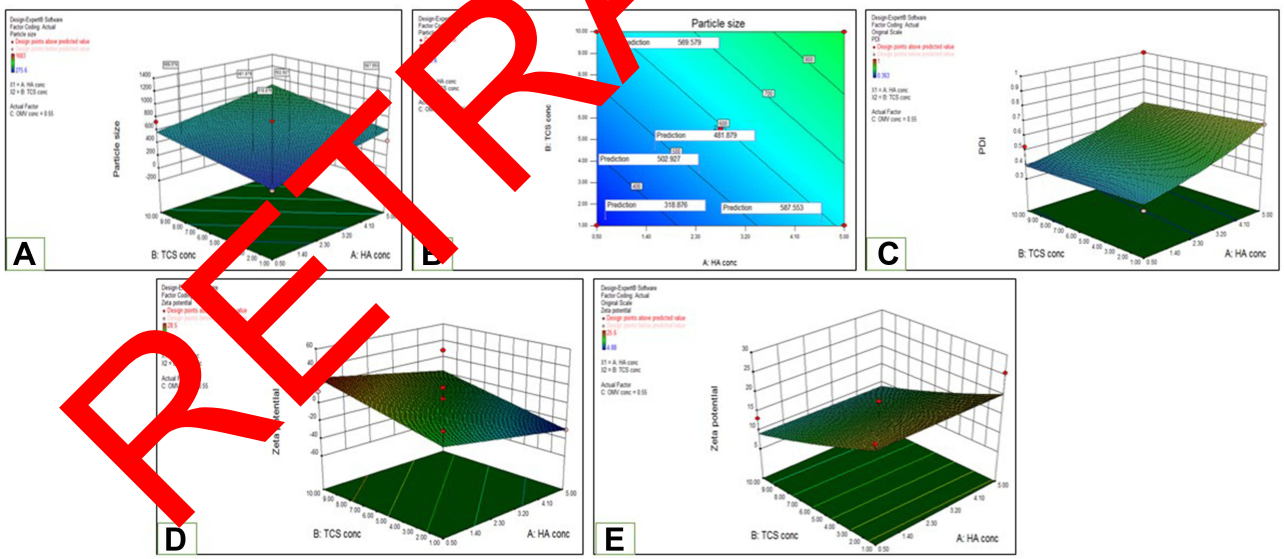

Figure 6 3D graphs via BoxBehnken factorial design of dependent variables particle size (**A** and **B**), PDI (**C**), and zeta potential (**D** and **E**) by using DOE responses for the optimization of HA-coated OMV-loaded NF.

Preparation of OMV-Loaded NFs

The HA-coated OMV-loaded TCs-NFs for comparison with the OMV vaccine strain were formed by following the ionic gelation method with the ionic bonding between the cationic amino group (-NH3+) of thiolated

chitosan and anionic HA molecule and were characterized for various morphological and physiological properties, as described below.

Physiochemical and Morphological Behavior

The extensive characterization of HA-coated OMV-loaded TCs-NFs was analyzed for various properties along with stability testing. The morphology of the prepared NFs had a spherical shape with good dispersion, but it did not have adhesion or subsidence damage. The measurement of these particles showed a fairly even distribution by a zeta sizer, and the outcomes for NFs after optimization are shown in Figure 7. In the current study, the minimum nanoparticle size for blank TCs-NF was 265.9 nm with a zeta potential of +22.3 mV and PDI of 0.225

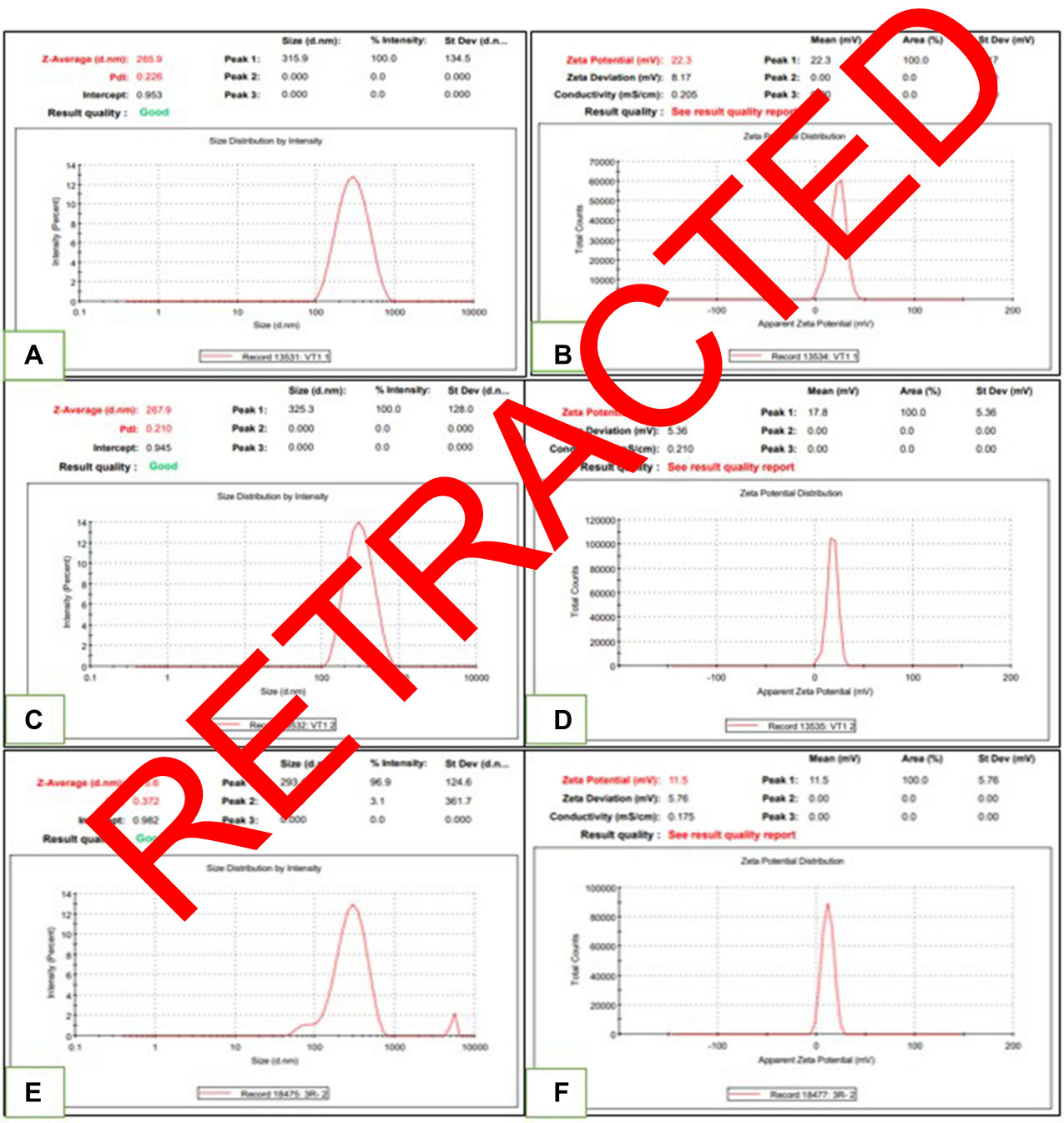

Figure 7 Blank NFs (**A** and **B**), OMV-loaded TCs (**C** and **D**), and HA-coated OMV-loaded TCs-NF (**E** and **F**) for their particle size, PDI, and zeta potential.

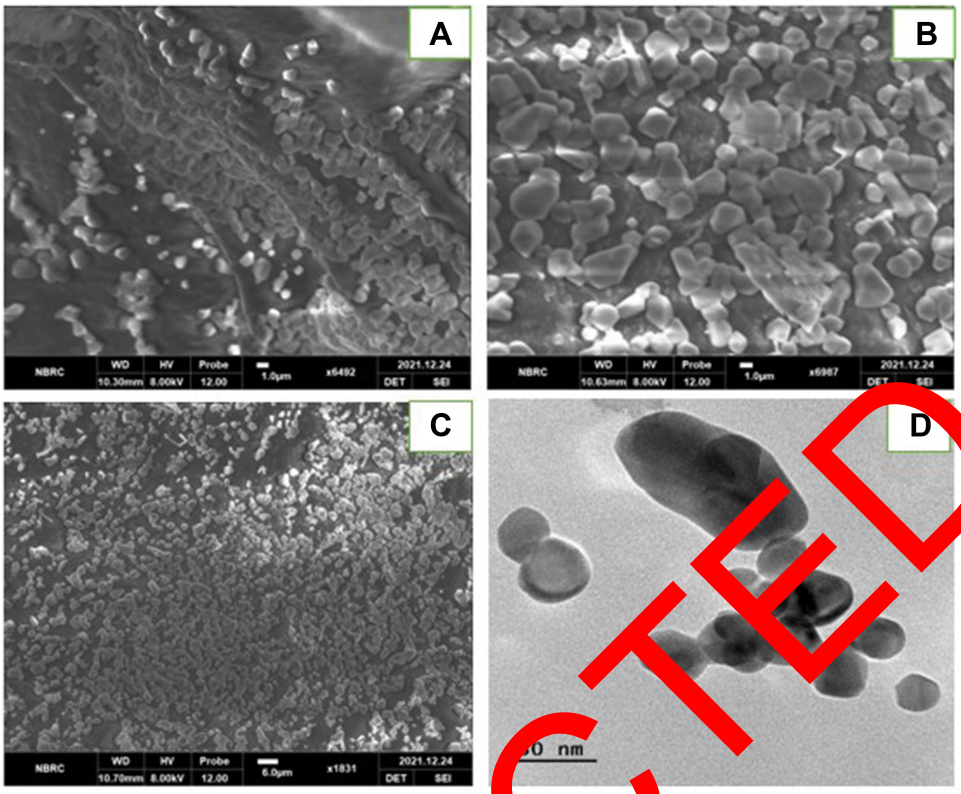

Figure 8 SEM images of blank NF temperatures (**A**) added TCs (**B**) and HA-coated OMV ded TCs (**C**) hile TEM image showed Nanosize particles of HA-coated OMV loaded TCs (**D**) at 50μm.

at the polymer concentration of 1.0 mg/mL. However, the NFs of OMV-loaded in TCs presented a slighter increase in mean nanoparticle size up to 267 nm with zeta potential +17.8 mV. When HA-coated OMV-loaded TCs-NF was analyzed, it showed a 2[illegible]6 nm average particle size with a zeta potential of +11.5 mV and PDI of 0.372 at the polymer (TCs) 1.0 mg/mL, TPP 0.5 mg/mL with a half dose (not less than 500 TCID units) of OMV.

The SEM analysis showed a smooth surface with spherical features (Figure 8A–C) and it was confirmed by Raman analysis by showing the highest peaks at 600 cm^{-1} because of the bending vibration of C-C-O bonds and the continuous decline was checked at approximately 950 cm^{-1}. The TEM analysis confirmed the virus encapsulation within nanoparticles which makes it very useful in targeted virus delivery systems (Figure 8D). The FTIR spectra indicated the hidden deflection at approximately 3,424 to 3,404 cm^{-1} because of the stretching of OH due to the presence of bands of TCs, at 2,900 to 2,880 cm^{-1} because of the stretching of CH, at 1,634 to 1,606 cm^{-1} because of the stretching of amide C=O in all formulations. The inclined stretching peak at the app. 2,496 cm^{-1} was observed in all NFs showing the presence of thiol (-SH) groups and confirming the successful thiolation of chitosan (Figure 9). The crystalline nature of the prepared formulation enclosing OMV was examined by the XRD phenomenon (Figure 9). The formulations went through high-temperature ranges from 50 and 300°C to check the thermal stability. The thermograms prepared by DSC showed that even after the thiolation of Cs, the NF encapsulating the OMV was not stable at high temperature.

Viral Quantification of NFs of OMV

Tissue Culture Infective Dose (TCID50)

A validation test was performed to calculate the TCID50 of prepared OMV-loaded NFs as compared to the commercially available MV vaccine at 7 p.d.i in PC3 cells. After calculating the proportionate distance (PD) between two dilutions by Reed and Munich, ID50 = 4.6. This refers to the dilution that would infect 50% of inoculated test units, known as

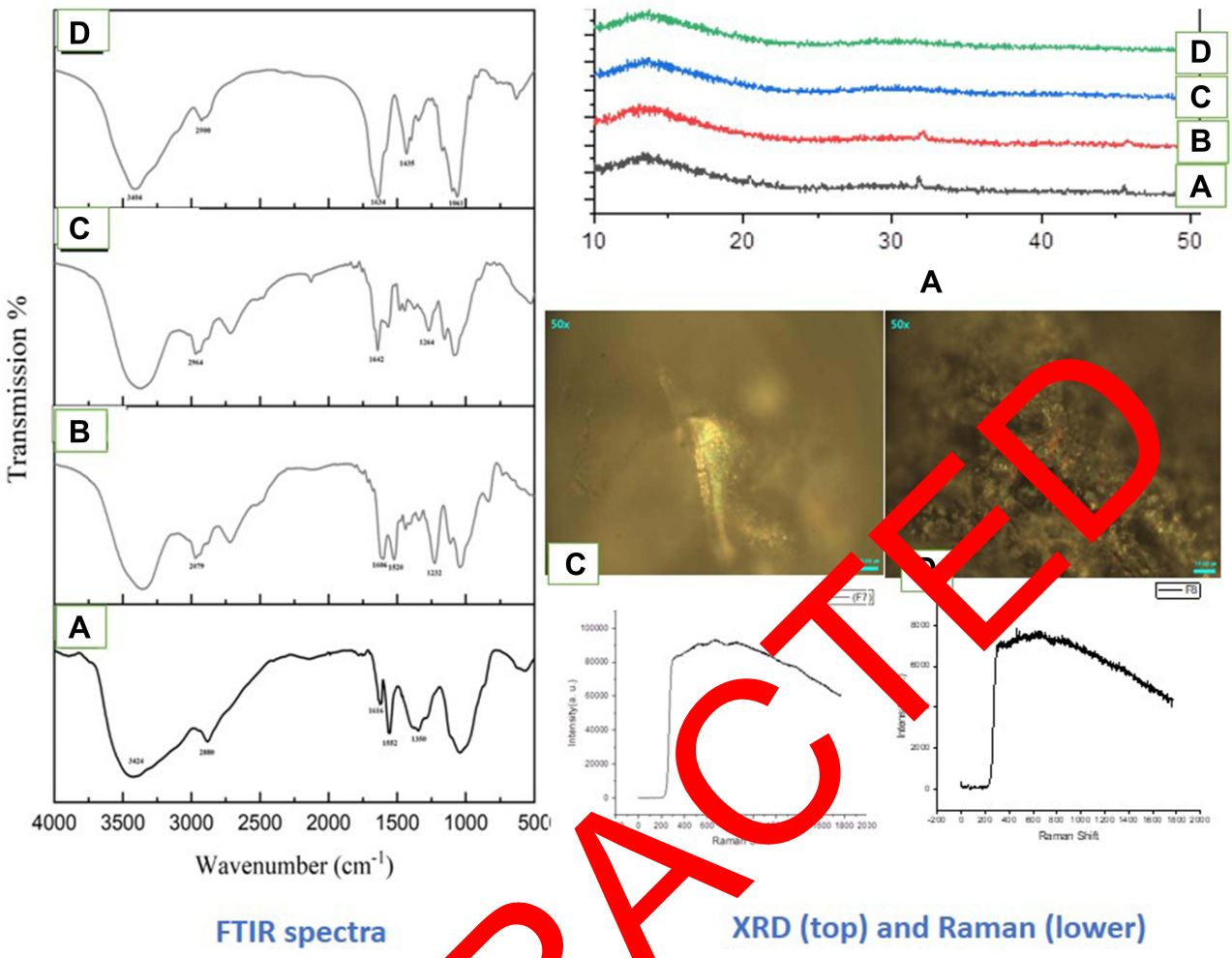

Figure 9 Spectrum obtained from FTIR of NF-TCs (**A**), Blank HA-coated TCs (**B**), OMV-loaded TCs (**C**), and HA-coated OMV-loaded TCs (**D**). XRD analysis (Top: Right) NFs of TCs (**A**), Blank HA-coated TCs (**B**), OMV-loaded TCs (**C**), and HA-coated OMV-loaded TCs (**D**). Raman analysis (Lower: Right) NFs OMV-loaded TCs (**C**), and HA-coated OMV-loaded TCs (**D**).

endpoint dilution. The virus titre in terms of TCID50 per unit volume was reciprocal titer units. As the viral inoculum was 0.1 mL, the titer of virus stock would be $1/10^{-4.6}/0.1=3.96x1$ titer ID50/mL for pure measles virus. For OMV-loaded TCs-NFs, ID50=10^{-5} and 2.5×10^{6} TCID50/mL but for HA-coated OMV-loaded TCs-NFs showed ID50=$10^{-6.37}$ and 2.34×10^{7} TCID50/mL.

Cytopathic Effects (CPE)

To investigate the cytopathic effect of OMV-loaded NFs and pure OMV for measuring the efficacy of NF. The cells were treated with different concentrations of 10, 50, and 100 µg/mL of 100 µL of NF and pure OMV for 24 hours (concentrations were adjusted for dilution factor). The cell morphology was analyzed using an inverted microscope at 12 and 24 hours with a 10x lens. The results exhibited that PC3 cells underwent apoptosis in a dose- and time-dependent manner. The least cytotoxicity was observed at 10 µg/mL. The concentration of 50 µg/mL showed a mild change in the shape of cells, while the highest toxicity was observed at 90 µg/mL, which was exhibited by rounding, detachment, and clumping of treated cells, as shown in Figure 10. The apoptosis induced in cells treated with OMV-loaded NFs was comparable to cells treated with a pure drug which confirms that prepared novel NFs can deliver virus efficiently maintaining its cytopathic effect while the targeted delivery capability of NF will spare normal cells from this toxic effect of the drug.

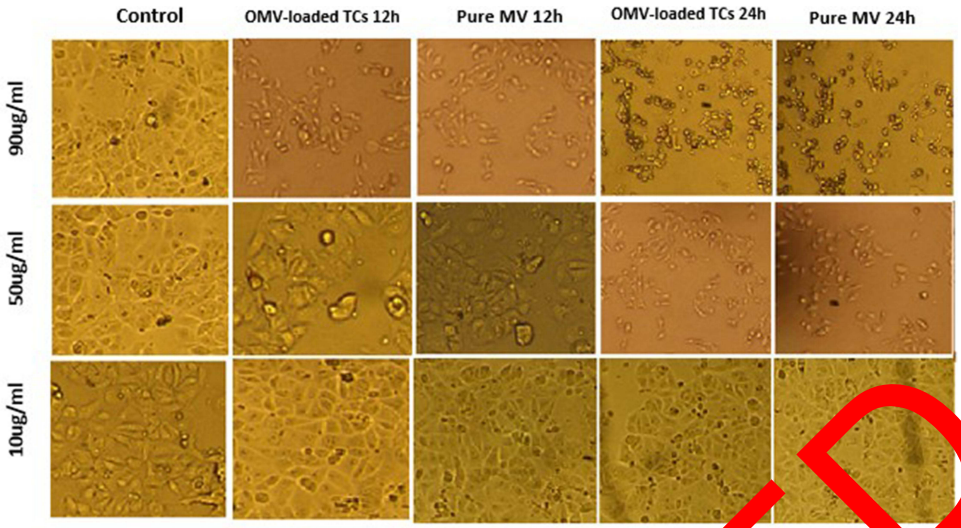

Figure 10 Change in cellular morphology of PC3 treated cells in time- and dose-dependent manner after the treatment with HA-coated OMV-loaded TCs compared with pure MV vaccine.

In vitro Virus Release of NFs

The release amount of virus from OMV-loaded NFs was completed for [illegible] hours, which indicated the sustained and continuous release of the virus as compared to commercially available MV vaccine solution. The experiment was repeated three times and, at each point, the data was measured in triplicate, as shown in Figure 11.

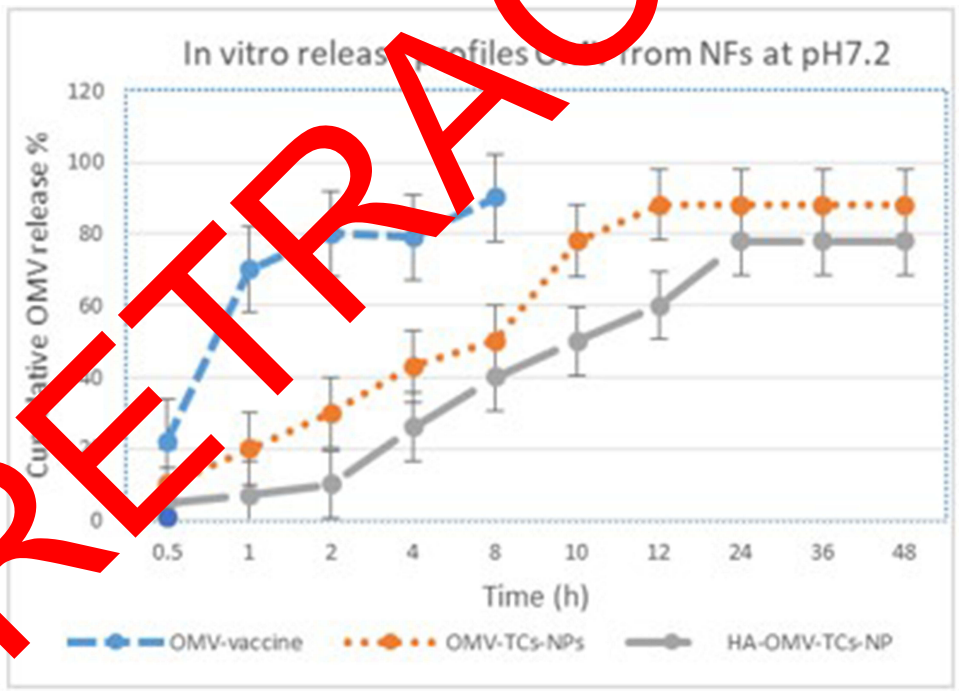

Figure 11 In vitro release profiles of virus from OMV-loaded NFs in PBS at pH 6.8. Mean values were analyzed using the Student's test. Data were presented as mean values of ±SD.

In vitro Anticancer Activity of OMV NFs

Cell Viability Analysis of OMV NFs

Prostate cancer cell line PC3 was inoculated at MOI (0.1, 0.5, 1, 3, 5, 10, 15, 20) of OMV- encapsulated NFs and the CPE was calculated for determination of the inhibitory dose 50 (IC50). MTT colorimetric assay was performed following 72 hours

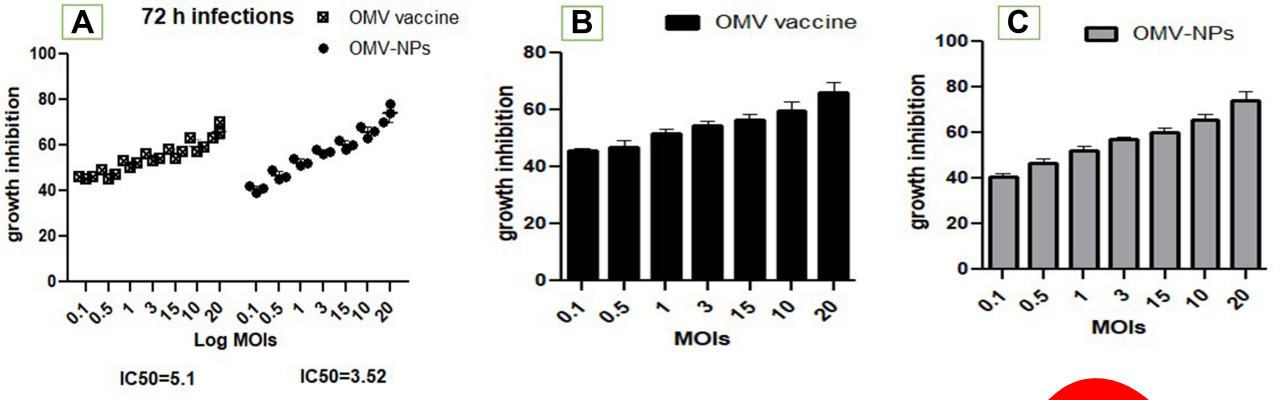

Figure 12 In vitro anti-cancer activity of the OMV vaccine and NFs on prostate cancer cell line PC3 for IC50 (**A**). The growth inhibition at different MOIs of OMV vaccine and NFs (**B** and **C**).

incubation time. IC50 and growth inhibition (GI) was evaluated by measuring the oncolytic effect of NF in treated and control cells. The results showed that OMV-loaded NF and OMV-vaccine have cytotoxic effects with IC50 of 3.52 and 5.1, respectively, on prostate cancer cell line (PC3) and the inhibition potential of a virus increased with an increase in MOI of the virus, as shown in Figure 12.

Stability Parameters

The stability parameters of the HA-coated OMV loaded TCs-NF were observed for variation in surface morphology, particle size, PDI, and zeta potential after 12 weeks of formulation. While the NF was stored at an ambient temperature of 37°C and refrigerated was °C along with oral measles vaccine. The liquid formulation exhibited an increase in particle size from 275.6 nm to 387.3 nm, zeta potential changed from ±11.5 mV to −23.7, and PDI changed from 0.372 to 0.591, while the lyophilized powder remained stable and did not exhibit any change after 3 months, as shown in Figure 13. Thus, virus-based nanoparticles are recommended to be stored in lyophilized powder for long-term storage and use.

The oral measles vaccine was extemporaneously diluted at the time of use with the diluent and then the zeta analysis was performed. It showed particle size 4[illegible]3.9 nm with PDI=0.363 and zeta potential was +16.4 mV. After 3 months of storage, particle size was increased to 1683 nm with PDI=1, and zeta potential was −24.0 mV, as shown in Figure 14. This data is vastly convincing that the liquid formulation of the vaccine strain was not stable for long-term storage at ambient temperature.

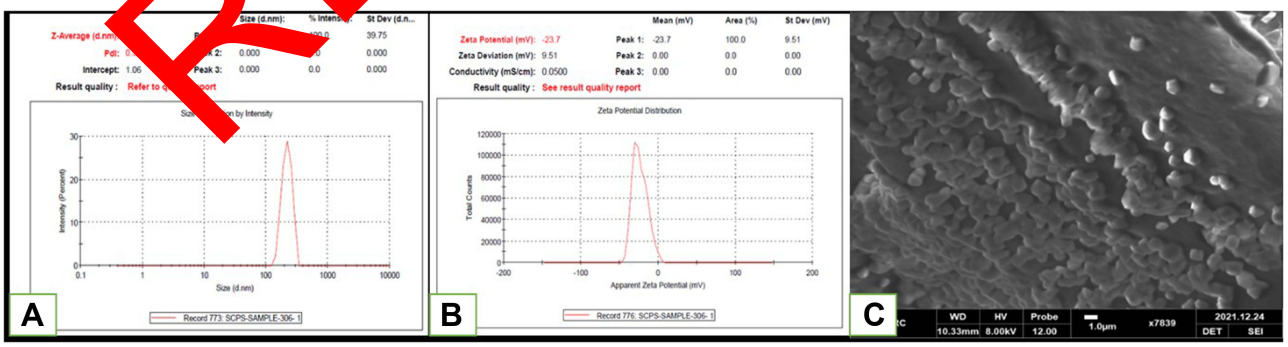

Figure 13 Zeta analysis of HA-coated OMV-loaded TCs liquid NF including particle size, PDI & zeta potential (**A** and **B**), and SEM of lyophilized NF (**C**) after 3 months storage.

Figure 14 Zeta analysis of oral measles vaccine liquid formulation including particle size, PDI, & zeta potential (**A** and **B**), and after 12 weeks of formulation, particle size, PDI, & zeta potential (**C** and **D**).

Discussion

Initially, the notion to use MV for the treatment of cancer patients ascended after reporting a case that linked measles disease to tumor reduction. Live weakened strain of MV strain was approved for vaccination in the 1960s after successful clinical trials and safety profile. After many years, experiments with various MV strains and their derivatives including Edmonston B, Moraten-Schwarz, Edmonston-Zagreb, AIK-C, rMVHu191, as well as Leningrad-16 cancer treatment have started and have shown strong oncolytic activity in preclinical data.[3] At the beginning of the studies, hematological malignancies were selected as targeted diseases. After further advances in research, solid tumors including breast, ovarian, prostate cancer, and brain tumors were found sensitive to the oncolytic activity of MV, while the healthy cells remain unharmed via this therapeutic moiety due to the presence of the natural lymphotropism of MV.[7] There is substantial data from previously published research demonstrating the preclinical efficacy of oncolytic MR for the treatment of various types of cancer. The exceptional safety parameters of the vaccine strains, no genotoxicity, and increased immunogenicity are advantages of oncolytic virus-based delivery systems. There are some specific challenges associated with MV including the activation of the immune system against viral disease, delivery of oncolytic MV to the targeted cells and unhindered oncolytic viro-immunotherapy.[31] One of the biggest problems faced after the system administration of the OV delivery system is escaping the humoral immune response of the patient. The neutralization of the virus happens before reaching the desired area in the presence of an immune system and circulating viral progeny become rapidly cleared by opsonization with the antibodies, complementary cascade, and coagulation factors present in the hepatic system resulting in sequestration by the mononuclear phagocytic system (MPS).

In this current research, a live attenuated oral measles vaccine (OMV) strain was used to formulate polymeric surface-functionalized ligand-based nanoformulation (NF). The surface functionalization of nanoparticles by ligand is one of the promising approaches for making the virus-based delivery system targeted rather than any genetic/structural modification and silencing of the viral capsid or genetic proteins. These ligands like hyaluronic acid protect the oncolytic OMV from antibody-mediated clearance. The NFs of HA-coated OMV-loaded TCs were extemporaneously formulated using the

ionic gelation method with the help of cross-linker TPP. No organic solvents or harsh chemicals are used that could destroy the virus or reduce its infectivity according to green synthesis protocols.[32]

Chitosan has exhibited the ability to activate macrophages and dendritic cells, and initiate cytokine release through binding with mannose receptor, and TLR4 (toll-like receptor). The presence of ionic interaction with the anionic membrane of cells, a cationic charge of chitosan supports its high uptake by Antigen Presenting Cells (APCs). This cationic interaction also promotes ionic binding with anionic DNA for vaccine delivery and antigens. According to the previous literature nanoparticles formulated with chitosan or its derivatives such as thiolated chitosan have shown more stability, adjustable cross-linking, controlled drug release, adhesion to biological surfaces, and cellular uptake than other vaccine delivery systems – such as liposomes, exosomes, and immune stimulating complexes. The increase in cellular uptake is due to the formation of both disulfide and covalent bonds between cysteine-rich mucosa and polymer, which is a more favorable binding interaction compared to electrostatic interactions of pure chitosan.[24]

Computational studies strongly stated the binding of HA with the CD44-R at both A & B binding sites from NFs of HA-coated TCs in prostate cancer cells. Furthermore, the host and viral protein–protein docking studies were performed and revealed significant interaction of viral hemagglutinin capsid protein with human caspase-I, NLRP3, and TNF- and interaction of the viral fusion protein with COX-II and caspase.[18,19] The NLRP3 inflammasome is a critical factor in activating the innate immune system, which promotes the activation of caspase-1. This activation further modulates the inflammatory cytokines and host immune mechanism against pathogenic microorganisms and cell damage by interfering with the pro-inflammatory cytokines. An inflammatory cytokine TNF-α is secreted by macrophages or monocytes during the phase of acute inflammation and it activates a cascade of signaling mechanisms within the cells resulting in necrosis or apoptosis, as shown in Figure 15.

The HA-coated OMV-loaded TCs-NFs prepared in our study demonstrated that the average particle size was 275.6 nm with PDI=0.372; these results further supplemented the previous outcomes published in 2010 by Prego and co-workers. They prepared the nanoparticles of chitosan with the particle size range of 160–200 nm with the ionic gelation method, after encapsulating the avian influenza virus in these NF, the particle size increased up to 397 nm.[33] Another study reported a particle size of about 80 nm for Chitosan NF and after the inclusion of the A/H1N1 influenza antigen, the nanoparticles range up to 106 nm.[34] In another work, loading a lentogenic vaccine strain of Newcastle disease virus into chitosan nanoparticles resulted in a 371 nm particle size. The variations in nanoparticle sizes can be attributed to the molecular weight of chitosan used, the thiolation rate and thiol group attached with chitosan, the volume ratio of chitosan to TPP solution, and the other preparation conditions including stir and sonication time, etc. which varied in each study.[35]

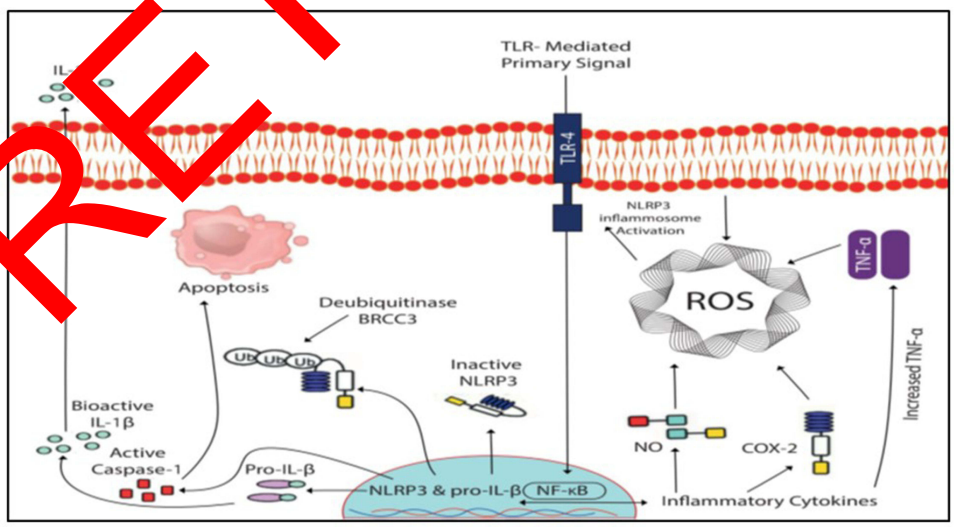

Figure 15 OMV intracellular pathways. 1) ligand binds to Toll-like receptor (TLR-4) which in turn activated NG-kB inside the nucleus releasing and increasing the concentration of inflammatory cytokines (TNF-A), COX2, and NO producing ROS that leads to the formation of NLRP3 inflammasome. 2) Inactive NLRP3 and pro-ILβ released from the nucleus bind deubiquitinase BRCC3 and caspases that cause apoptosis of the cancer cell.

The applications of NFs are dependent on their nanoparticle size, charge quantity, and distribution in the cells which affect the loading, encapsulation, and release of the drug, in vitro and in vivo authenticity, prepared formulation toxicity profile, and stability parameters. Small-sized nanoparticles have a high surface-to-volume ratio and rapidly release the encapsulated material as they adhere to the surface of the cell membrane.[24]

OMV-loaded TCs-NF zeta potential decreased from ±17.8 mV to ±11.5 mV after coating with HA, similar surface charge measurements related outcomes were shown by Prego with co-workers in 2010.[33] They also stated that the surface charge in recombinant hepatitis B surface antigen-loaded in chitosan nanoparticles was decreased as compared to the blank nanoparticles from 30 mV to 5.9 mV. Another study reported 4.29 mV zeta potential after encapsulation of AIV in chitosan nanoparticles. When the vaccine strain of NDV was encapsulated in chitosan, the nanoparticles showed 2.84 mV zeta potential, inducing better protection of immunized SPF chickens than the live NDV LaSota vaccine strain and the inactivated NDV vaccine.[35] The reduction in surface charge achieved in the current study after encapsulation of OMV in HA-coated NF may be due to the effect of the neutralization with the negatively charged antigen that decreases the zeta potential of TCs nanoparticles as compared to chitosan nanoparticles alone. The cationic NPs are reported to display higher uptake by direct permeation in comparison with neutral or anionic NPs.[11]

In recent reports, the inactivated Rift Valley Fever Virus (RVFV) loaded into chitosan-based nanoparticles that were formulated by ion gelation were investigated for its humoral and cell-mediated immune response against infection.[36] The OMV nanoparticles were tested against BT-474 and MDA-MB-468 breast cancer cells and proved a very potential therapeutic candidate in cancer treatment.[37] It was previously published that the charged nanoparticles showed a higher clearance rate from systemic circulation as compared to neutral particles and the high positive zeta potential promotes the scavenging of the nanoparticles by anionic acidic cancer cells. Oncolytic virus nanoparticles, including foot-and-mouth disease virus (FMD), were fabricated using chitosan (CS) into a 281.2 nm size and with a 13 mV positive electrical charge to assess the anti-fungal potential for mucosal vaccine.[38–40]

According to the results of our study, the titer of the encapsulated virus was calculated to be 2.34×107 TCID50/mL units, showing the formation of syncytia in infected after day 7. At MOIs 0.1, 0.5, 1, 3, 5, 10, 15, and 20 of the HA-coated OMV-loaded NFs as compared to the OMV vaccine were inoculated on prostate cancer cell lines (PC3, an androgen receptor-independent cells) with an IC50 of 5 and 3.52, respectively. Growth inhibition of PC3 cells was observed after the 72 hour incubation period via MTT assay showing apoptotic cell death of the cancer cells. Our outcomes explained that the HA-coated OMV-loaded TCs-NF had higher oncolytic activity compared with the commercially available OMV vaccine in vitro. We have reported several novel findings regarding the viral-delivery system of polymer-coated with biocompatible material after encapsulating live attenuated virus strain from a commercial vaccine.

Conclusion

The current investigation was carried out to enhance the efficacy and immunotherapeutic potential of OMV with a surface functionalizing ligand. The live attenuated vaccine strain from OMV was loaded into a thiolated chitosan nanoformulation coated with Hyaluronic acid which was prepared by ionic gelation method with green synthesis protocol without using any organic solvent/harsh material for targeted oncolytic viral delivery. Prostate cancer (PC3) AR-independent aggressive cells produce less PSA and spread outside the prostate earlier were chosen to check the efficacy of the prepared nanoformulation at different MOIs in cell culture systems. The NF produced, with a particle size in the 200–300 range, has a less positive zeta potential that favors measles virus uptake by anionic cancer cells at acidic pH. It has shown good stability with an excellent sustained release profile. Furthermore, these formulations showed significant comparable growth inhibition with commercially available oral measles vaccine ($p<0.05$) after quantification of a significant amount of encapsulated virus titer and active viral progeny. All of these properties enhance the potency, efficacy, and active targeting of NFs of OMV as a strongly targeted immunomodulator in cancer therapeutics. The key advantage of sustained-release virus-based systems is to minimize the adverse effects of therapeutic moiety by widening the range between the lowest effective and toxic dose. We hypothesized that this approach can increase patient compliance by decreasing the frequency of drug administration and reducing the overall regimen with increased on-target efficacy. These outcomes will be further supported by extensive in vitro and in vivo experiments.

Ethical Approval

This study does not need ethical approval.

Disclosure

The authors declare no conflict of interest in this study.

References

1. Naseer F, Ahmad T, Gul R, Anjum S. Serendipity for the intervention of COVID-19 and Prostatic Adenocarcinoma (PaC) pros. *Cancer Prostatic Dis*. 2022;10:1–3.
2. Naseer F, Ahmad T, Kousar K, Anjum S. Advanced therapeutic options for treatment of metastatic castration-resistant prostatic adenocarcinoma. *Front Pharmacol*. 2021;12:728054. doi:10.3389/fphar.2021.728054
3. Mariadoss A, Vinayagam R, Senthilkumar V, et al. Phloretin loaded chitosan nanoparticles augments the pH-dep[illegible]ent mitocho[illegible]rial-mediated intrinsic apoptosis in human oral cancer cells. *Int J Biol Macromol*. 2019;130:997–1008. doi:10.1016/j.ijbiomac.2[illegible]9.03.031
4. Sebastian R. Nanomedicine-the future of cancer treatment: a review. *J Cancer Prev Curr Res*. 2017;8. doi:10.15406/[illegible]ccr.2017.08.0[illegible]265
5. Msaouel P, Iankov ID, Dispenzieri A, Galanis E. Attenuated oncolytic measles virus strains as cancer therapeutics. *Curr Pha[illegible] Biotechnol*. 2012;13(9):1732–1741. doi:10.2174/138920112800958896
6. Ammour Y, Ryabaya O, Amouretinina Y. The susceptibility of human melanoma cells to infection w[illegible] the leni[illegible]ad-16 vaccine strain of measles virus. *Viruses*. 2020;12(2):173. doi:10.3390/v12020173
7. Engeland C, Ungerechts G. Measles virus as an oncolytic immunotherapy. *Cancers*. 2021;13([illegible]:544. doi:[illegible]3390/can[illegible]s13030544
8. Cook M, Chauhan A. Clinical application of oncolytic viruses: a systematic review. *Int J [illegible]Sci*. 2020;12(2[illegible]75[illegible] doi:10.3390/ijms21207505
9. Leichner C, Jelkmann M, Bernkop-Schnürc A. Thiolated polymers: bioinspired polymer[illegible]utilizi[illegible]ne of the mos[illegible]mportant bridging structures in nature. *Adv Drug Deli Rev*. 2019;9:191–221.
10. Grosso R, de-Paz M. Thiolated-polymer-based nanoparticles as an avant-garde ap[illegible]or anticancer [illegible]rapies: reviewing thiomers from chitosan and hyaluronic acid. *Pharmaceutics*. 2021;13:854. doi:10.3390/pharmaceutics[illegible]060854
11. Yanat M, Schroen K. Preparation methods and applications of chitosan nan[illegible]particles; with[illegible] outlook toward reinforcement of biodegradable packaging. *Reac Funct Polymers*. 2021;161:1048–1049.
12. Naseer F, Ahmed M, Majid A, Kamal W, Phulle A. Green nanoparticles as mu[illegible]unctional na[illegible]medicines: insights into anti-inflammatory effects, growth signalling and apoptosis mechanism in cancer. *Sem Cance[illegible]Biol*. 2022;3:[illegible]
13. Sandhya J, Veeralakshmi S, Kalaiselvam S. Tripolyphosphate cro[illegible]lin[illegible]Triticum aestivum (wheatgrass) functionalized antimicrobial chitosan: ameliorating effect on physicochemical, mechanical, invitro cy[illegible]compat[illegible]and cell migration properties. *J Biomol Struct Dynamics*. 2020;2020:1–10.
14. Li W, Cohen A, Sun Y, et al. The role of CD44 in gl[illegible]se [illegible]etabolis[illegible]n prostatic small cell neuroendocrine carcinoma. *Mol Can Res*. 2016;14 (4):344–353. doi:10.1158/1541-7786.MCR-15-046[illegible]
15. Li W, Qian L, Lin J. CD44 regulates prosta[illegible]cancer p[illegible]feration, [illegible]vasion, and migration via PDK1 and PFKFB4. *Oncotarget*. 2017;8 (39):65143–65151. doi:10.18632/oncotarget.[illegible]7821
16. Padhi S, Behera A, Hasnain S, Nayak A. [illegible]itosan-ba[illegible] drug delivery systems in cancer therapeutics. *Chit Drug Deliv*. 2022;2022:159–193.
17. Mattheolabakis G, Milane L, Amit S, [illegible]poor M. Hyalu[illegible]ic acid targeting of CD44 for cancer therapy: from receptor biology to nanomedicine. *J Drug Target*. 2015;23:605–618. d[illegible]10.3[illegible]/1061186X.20[illegible].1052072
18. Desta I, Porter K, Xia B, Kozakov D, Vajda S. [illegible]formance and its limits in rigid-body protein-protein docking. *Structure*. 2020;28(9):1071–81. e3. doi:10.1016/j.str.2020.06.006
19. Vajda S, Yueh C, Beglov [illegible], Bohnuud T, Mottarella S, Xia B. New additions to the ClusPro server motivated by CAPRI. *Proteins*. 2017;85 (3):435–444. doi:10.10[illegible]prot.252[illegible]
20. Tahara M, Ohno S, Sakai [illegible]Ito[illegible], Fukuhara H, Komase K. The receptor-binding site of the measles virus hemagglutinin protein itself constitutes a conserved neutr[illegible]ng epit[illegible]. *J Virol*. [illegible]13;87(6):3583–3586. doi:10.1128/JVI.03029-12
21. Miao E, Leaf I, Treuting P, Mao [illegible], Do[illegible]M, Sarkar A. Caspase-1-induced pyroptosis is an innate immune effector mechanism against intracellular bacteria. *Nat Immunol*. 2010;11(12):[illegible]136–1142. doi:10.1038/ni.1960
22. Lupfer C, [illegible]nnegan[illegible]ole of inflammasome modulation in virulence. *Virulence*. 2012;3(3):262–270. doi:10.4161/viru.20266
23. Minor D. Li[illegible]tenuated vaccines: historical successes and current challenges. *Virology*. 2015;5:379–392. doi:10.1016/j.virol.2015.03.032
24. Naseer F, Ahma[illegible]T, Kousar K, Kakar S, Gul G, Anjum S. Formulation of surface-functionalized hyaluronic acid-coated thiolated chitosan nano-formulation f[illegible]he delivery of vincristine in prostate cancer: a multifunctional targeted drug delivery approach. *J Drug Deliv SciTechnol*. 2011;74:1035–1045.
25. Payne S. Methods to study viruses. *Viruses*. 2017;2017:37–52.
26. Cromeans T, Lu X, Erdman D, Humphrey C, Hill V. Development of plaque assays for adenoviruses 40 and 41. *J Virol Methods*. 2008;151:140–145. doi:10.1016/j.jviromet.2008.03.007
27. Barretto N, Uprichard S. Hepatitis C virus cell-to-cell spread assay. *Bio Protocol*. 2014;4(24):e1365. doi:10.21769/BioProtoc.1365
28. Saleem M, Naseer F, Ahmad S, Baig K, Irshad I. In vivo cytotoxic effects of methanol extract of Convolvulus arvensis on 7-12-dimethyl Benz(a) anthracene (DMBA) induced skin carcinogenesis. *Afr J Pharm Pharmacol*. 2015;9(12):397–404. doi:10.5897/AJPP2014.4165
29. Jalilian M, Derakhshandeh K, Kurd M, Lashani H. Targeting solid lipid nanoparticles with anisamide for docetaxel delivery to prostate cancer: preparation, optimization, and in-vitro evaluation. *Iran J Pharm Res*. 2021;20(1):327–338. doi:10.22037/ijpr.2020.113436.14302
30. Ghaferi M, Amari S, Mohrir B, Raza A, Shahmabadi H, Alavi S. Preparation, characterization, and evaluation of cisplatin-loaded polybutylcyanoacrylate nanoparticles with improved in vitro and in vivo anticancer activities. *Pharmaceuticals*. 2020;13(3):44. doi:10.3390/ph13030044
31. Mühlebach M. Measles virus in cancer therapy. *Curr Opin Virol*. 2020;41:85–97. doi:10.1016/j.coviro.2020.07.016

32. Boroumand H, Badie F, Mazaheri S, et al. Chitosan-based nanoparticles against viral infections. *Front Cell Infect Microbiol*. 2021;11:643953. doi:10.3389/fcimb.2021.643953
33. Prego C, Paolicelli P, Díaz B, Vicente S, Sánchez A, González-Fernández A. Chitosan-based nanoparticles for improving immunization against hepatitis B infection. *Vaccine*. 2010;28:2607–2614. doi:10.1016/j.vaccine.2010.01.011
34. Dzung N, Ha N, Van D, Phuong N, Quynh N, Hiep D. Chitosan nanoparticle as a novel delivery system for A/H1n1 influenza vaccine: safe property and immunogenicity in mice. *World Acad Sci Eng Technol*. 2011;60:1839–1846.
35. Zhao K, Chen G, Shi X, Gao T, Li W, Zhao Y. Preparation and efficacy of a live Newcastle disease virus vaccine encapsulated in chitosan nanoparticles. *PLoS One*. 2012;7:e53314. doi:10.1371/journal.pone.0053314
36. El-Sissi A, Mohamed F, Danial N, Gaballah A, Ali K. Chitosan and chitosan nanoparticles as an adjuvant in local Rift Valley Fever inactivated vaccine. *Biotechnology*. 2020;10(3):88.
37. Liu C, Wong S, Tai C, et al. Ursolic acid and its nanoparticles are potentiators of oncolytic measles virotherapy against breast cancer cells. *Cancers*. 2021;13(1):136. doi:10.3390/cancers13010136
38. Tajdini F, Amini M, Rezaei A, Azimi M. Foot and mouth disease virus-loaded fungal chitosan nanoparticles for intranasal administration: impact of formulation on physicochemical and immunological characteristics. *Pharma Dev Technol*. 2014;3:21–29.
39. Tran S, DeGiovanni P, Piel B, Rai P. Cancer nanomedicine: a review of recent success in drug delivery. *Clin Transl Med*. 2017;6:44. doi:10.1186/s40169-017-0175-0
40. Kousar K, Ahmad T, Naseer F, Kakar S, Anjum S. Review article: immune landscape and immunotherapy options in cervical carcinoma. *Cancers*. 2022;14:4458. doi:10.3390/cancers14184458